



CHALMERS
UNIVERSITY OF TECHNOLOGY

Development of an Haa1-based biosensor for acetic acid sensing in *Saccharomyces cerevisiae*

Downloaded from: <https://research.chalmers.se>, 2025-12-04 22:50 UTC

Citation for the original published paper (version of record):

Mormino, M., Siewers, V., Nygård, Y. (2021). Development of an Haa1-based biosensor for acetic acid sensing in *Saccharomyces cerevisiae*. *FEMS Yeast Research*, 21(6).
<http://dx.doi.org/10.1093/femsyr/foab049>

N.B. When citing this work, cite the original published paper.

RESEARCH ARTICLE

Development of an Haa1-based biosensor for acetic acid sensing in *Saccharomyces cerevisiae*

Maurizio Mormino¹, Verena Siewers^{1,2} and Yvonne Nygård^{1,*†}

¹Department of Biology and Biological Engineering, Chalmers University of Technology, SE-412 96 Gothenburg, Sweden and ²Novo Nordisk Foundation Center for Biosustainability, Chalmers University of Technology, SE-412 96 Gothenburg, Sweden

*Corresponding author: Department of Biology and Biological Engineering, Chalmers University of Technology, Kemivägen 10, SE-412 96 Gothenburg, Sweden. Tel: +46317726868; E-mail: yvonne.nygard@chalmers.se

One sentence summary: Development, characterization and application of a biosensor for sensing acetic acid in yeast.

Editor: Zongbao Zhao

†Yvonne Nygård, <http://orcid.org/0000-0001-6117-0343>

ABSTRACT

Acetic acid is one of the main inhibitors of lignocellulosic hydrolysates and acetic acid tolerance is crucial for the development of robust cell factories for conversion of biomass. As a precursor of acetyl-coenzyme A, it also plays an important role in central carbon metabolism. Thus, monitoring acetic acid levels is a crucial aspect when cultivating yeast. Transcription factor-based biosensors represent useful tools to follow metabolite concentrations. Here, we present the development of an acetic acid biosensor based on the *Saccharomyces cerevisiae* transcription factor Haa1 that upon binding to acetic acid relocates to the nucleus. In the biosensor, a synthetic transcription factor consisting of Haa1 and BM3R1 from *Bacillus megaterium* was used to control expression of a reporter gene under a promoter containing BM3R1 binding sites. The biosensor did not drive expression under a promoter containing Haa1 binding sites and responded to acetic acid over a linear range spanning from 10 to 60 mM. To validate its applicability, the biosensor was integrated into acetic acid-producing strains. A direct correlation between biosensor output and acetic acid production was detected. The developed biosensor enables high-throughput screening of strains producing acetic acid and could also be used to investigate acetic acid-tolerant strain libraries.

Keywords: biosensor; acetic acid; Haa1; synthetic transcription factor

INTRODUCTION

Industrial bioproduction processes require strains that are tolerant to stress conditions and that can utilize nonfood raw materials such as lignocellulosic biomasses, which often contain compounds that are inhibitory to the cells. Tolerance toward inhibitors such as acetic acid that is released during biomass hydrolysis is crucial for yeast cell factories to be used in biorefineries. While significant effort has been put into developing more robust yeast strains, tolerance to acetic acid remains a

bottleneck for the development of second-generation bioprocesses (Robak and Balcerak 2018). Tolerance to lignocellulosic hydrolysates greatly varies between different *Saccharomyces cerevisiae* strains (van Dijk *et al.* 2020), and depending on feedstock and pretreatment employed, the acetic acid concentration in lignocellulosic hydrolysates may range from 1 to 15 g L⁻¹ (~17–250 mM) (Palmqvist and Hahn-Hägerdal 2000; Klinke 2004). For a recent review on acetic acid stress in yeast, we refer to Guaragnella and Bettiga (2021).

Received: 30 June 2021; Accepted: 1 September 2021

© The Author(s) 2021. Published by Oxford University Press on behalf of FEMS. This is an Open Access article distributed under the terms of the Creative Commons Attribution-NonCommercial License (<https://creativecommons.org/licenses/by-nc/4.0/>), which permits non-commercial re-use, distribution, and reproduction in any medium, provided the original work is properly cited. For commercial re-use, please contact journals.permissions@oup.com

Acetic acid can, in its protonated form, freely pass the lipid bilayer of the yeast cell membrane (Casal, Cardoso and Leão 1996). Once in the cytosol, the acetic acid dissociates, releasing protons that need to be extruded from the cell at the cost of cellular energy (Pampulha and Loureiro-Dias 1990). Exposure to high concentrations of acetic acid can cause acidification of the cell, growth retardation and even loss in cell viability (Mira, Becker and Sá-Correia 2010a; Guaragnella et al. 2011; Giannatasio et al. 2013), as dissociated acids cannot diffuse through the cell membrane (Pampulha and Loureiro-Dias 1990). Acetic acid export is still today not very well understood, while acetic acid stress has been shown to lead to genome-wide responses, including regulation of central metabolic fluxes, vesicle formation processes and proteasomal degradation pathways (Dong et al. 2017; Mukherjee et al. 2021).

Acetic acid is fundamental to all cells, as part of acetyl-coenzyme A (acetyl-CoA), a molecule central to many biochemical reactions in protein, lipid and carbohydrate metabolism (Jeukendrup 2002; Jell et al. 2007). Acetyl-CoA is also a key precursor metabolite for numerous industrially relevant products. While novel technologies such as CRISPR-Cas9-based genome editing have significantly speeded up the engineering of cells, the evaluation of resulting phenotypes and product synthesis often remains a bottleneck in metabolic engineering (Qiu, Zhai and Hou 2019). Therefore, tools to monitor inhibitory compounds or metabolites are needed to advance the development of industrial production strains. Biosensors that can be used for strain evaluation and high-throughput screening can accelerate the classic design-build-test-learn cycle and provide powerful tools for advancing the use of *S. cerevisiae* as a cell factory (Qiu, Zhai and Hou 2019).

Various biosensors, often based on inducible promoters or transcription factors (TFs), have been demonstrated for yeast. These molecular devices have been employed to monitor a wide range of molecules (metals, sugars, acids, etc.) as well as for optimization and control of metabolic pathways (Qiu, Zhai and Hou 2019). Several TF-based biosensors, where binding sites (BSs) of a specific metabolite-responsive TF are inserted into a promoter driving a reporter, have in recent years been developed for *S. cerevisiae*. In such biosensors, the presence of the sensed compound activates the expression of a reporter gene, which generates a measurable output (e.g. fluorescence) that ultimately describes the target compound concentration. Yeast biosensors often use heterologous, bacterial TFs as a starting point (Qiu, Zhai and Hou 2019), while only a few yeast biosensors based on eukaryotic TFs have been reported (Bovee et al. 2007; Chou and Keasling 2013; Feng et al. 2015). Still, many endogenous yeast TFs are known to bind specific ligands and thereby regulate target genes in response to changing conditions.

The zinc-finger TF Haa1 plays a central role in regulating the cellular response to weak acid stress (Collins, Black and Liu 2017) and it has been shown to directly bind acetic acid ions in the cytoplasm (Kim et al. 2018). Upon exposure to lactic (Sugiyama et al. 2014) or acetic (Collins, Black and Liu 2017) acid, Haa1 relocates to the nucleus. The phosphorylation of Haa1 is reported to play a crucial, yet not fully understood, part in the relocation process. Haa1 was reported to get dephosphorylated or mildly phosphorylated after lactic or acetic acid exposure, respectively (Sugiyama et al. 2014; Collins, Black and Liu 2017). Furthermore, it has been shown that mutations in *HRR25* (encoding a casein kinase) lead to reduced Haa1 phosphorylation, increased Haa1 nuclear localization and activation of Haa1 target gene expression, suggesting that phosphorylation of Haa1 plays a central role in Haa1-dependent gene regulation (Collins, Black and Liu

2017). Upon weak acid exposure, Haa1 regulates a large set of genes encoding enzymes involved in different processes such as protection against acids and lipid, carbohydrate and amino acid metabolism, protein folding and nucleic acid processing (Mira, Becker and Sá-Correia 2010a; Mira, Teixeira and Sá-Correia 2010b; Sugiyama et al. 2014).

In the present study, we report the design, characterization and utilization of an Haa1-based biosensor that senses acetic acid concentration and production in *S. cerevisiae* cultures. The acetic acid biosensor was integrated into a set of strains that were genetically engineered to produce different levels of acetic acid, demonstrating the possibility to use the biosensor as a tool for screening purposes. Beyond the utility of the biosensor itself, our results offer novel insight in the role of Haa1 in response to weak acids.

MATERIALS AND METHODS

Yeast strains and cultivation conditions

Yeast strains used in the study are listed in Table 1. For construction of the biosensor, *S. cerevisiae* CEN.PK113-5D (Entian and Kötter 2007) was used as the parental strain. The yeast cells were cultivated in synthetic defined (SD) medium (0.77 g L⁻¹ complete supplement mixture [CSM] drop out, 6.9 g L⁻¹ yeast nitrogen base without amino acids [YNB w/o AA], 20 g L⁻¹ glucose, pH 5.5 or 3.5), in white 96-well plates (Greiner CELLSTAR®, Sigma-Aldrich, St Louis, MO, USA) with 200 or 250 µL culture or in 100-mL shake flasks with 20 mL culture, inoculated from a preculture (5 mL, grown overnight in SD media at pH 5.5) to an OD₆₀₀ of 0.1. Acetic acid, as well as other acids used, was added to the media at the beginning of the cultivation, or after 5, 10, 24 or 48 h. All acids except lactic acid were dissolved (powders) or diluted (liquid solutions) in distilled water to the concentration of 1 M before being added to the media. Lactic acid was diluted in distilled water to a final concentration of 5 M before being added to the medium. For microscopy analysis and yMM2.9 characterization, the pH of the acetic acid was adjusted to the pH of the medium through NaOH titration. Plates with 200 µL cultures were cultivated at 30°C and 85% humidity, shaking at 995 rpm, using a microreactor device (BioLector, m2p-laboratories GmbH, Baesweiler, Germany). Plates with 250 µL cultures were cultivated at 30°C, shaking at 250 rpm, using another screening device (Growth Profiler 960, EnzyScreen, Heemstede, The Netherlands). Flask cultures were incubated at 30°C and 220 rpm in shakers.

Design of constructs, modular cloning and strain construction

All genetic constructs were cloned following the MoClo method (Lee et al. 2015). *Escherichia coli* DH5α was used for plasmid construction and grown in lysogeny broth (LB), composed of 5 g L⁻¹ yeast extract, 10 g L⁻¹ peptone from casein and 10 g L⁻¹ NaCl. Agar-agar was added at 16 g L⁻¹ to make LB plates. The sequences of all primers and plasmids used for strain construction and verification are listed and described in Tables S1–S3 (Supporting Information). The primers were purchased from Eurofins Genomics (Ebersberg, Germany), and PCR components from Thermo Scientific (Waltham, MA, USA). Plasmids were purified using the GeneJET Plasmid Miniprep Kit (Thermo Scientific).

New level-0 genetic parts containing BM3R1 (Rantasalo et al. 2018), BM3R1 BSs followed by the *ENO1* core promoter

Table 1. List of yeast strains used in this study.

Strain	Description	Function	Parental strain	Origin
CEN.PK113-5D	MATa <i>ura3-52 TRP1 LEU2 HIS3</i>	Parental strain		Entian and Kötter (2007)
IMX581	MATa <i>ura3-52 can1Δ::cas9-natNT2 TRP1 LEU2 HIS3</i>	Parental strain		Mans et al. (2015)
JH18	IMX581 <i>tkl1/2Δ tal1Δ nqm1Δ pho13Δ SHB17p::TDH3p XII-1::TEF1p-Xfpk-ADH1t</i>	Parental strain	IMX581	Hellgren et al. (2020)
JH24	IMX581 <i>tkl1/2Δ tal1Δ nqm1Δ pho13Δ SHB17p::TDH3p XII-1::TEF1p-Xfpk-ADH1t XI-1::eTDH3p-Xfpk-CYC1t X-2::eTEF1p-pta-CYC1t</i>	Parental strain	IMX581	Hellgren et al. (2020)
JH29	IMX581 <i>tkl1/2Δ tal1Δ nqm1Δ pho13Δ SHB17p::TDH3p XII-1::TEF1p-Xfpk-ADH1t XI-1::eTDH3p-Xfpk-CYC1t X-2::eTEF1p-pta-CYC1t gpp1Δ X-4::Hxt7p-ACC1** XI-3 HXT7p-mcrC + TEF1p-mcrN</i>	Parental strain	IMX581	Hellgren et al. (2020)
JH37	IMX581 <i>XII-1::TEF1p-Xfpk-ADH1t XI-1::eTDH3p-xfpk-CYC1t X-2::eTEF1p-pta-CYC1t gpp1Δ X-4::Hxt7p-ACC1** XI-3 eTDH3p-mcr</i>	Parental strain	IMX581	Hellgren et al. (2020)
mRuby2+	CEN.PK113-5D <i>RPL13A::RPL13A-mRuby2</i>	Control	CEN.PK113-5D	This study
yMM1.11	CEN.PK113-5D	Control	CEN.PK113-5D	This study
	HO::HREsYGP1p-mCherry-ScSSA1t			
yMM1.12	CEN.PK113-5D HO::	Control	CEN.PK113-5D	This study
	BM3R1_BSsENO1cp-mCherry-ScSSA1t			
yMM1.13	CEN.PK113-5D	Control	CEN.PK113-5D	This study
	HO::HAA1p-BM3R1-mTurquoise2-ScSSA1t			
yMM1.15	CEN.PK113-5D HO::TDH3p-mCherry-ScSSA1t	Control	CEN.PK113-5D	This study
yMM1.17	CEN.PK113-5D	Control	CEN.PK113-5D	This study
	HO::TDH3p-mTurquoise2-ADH1t			
yMM2.4	CEN.PK113-5D	Biosensor	CEN.PK113-5D	This study
	HO::HAA1p-HAA1-mTurquoise2-scENO1t-YGP1p-mRuby2-ScSSA1t			
yMM2.9	CEN.PK113-5D HO::HAA1p-BM3R1-HAA1-mTurquoise2-scENO1t-BM3R1_BSsENO1cp-mCherry-ScSSA1t	Biosensor	CEN.PK113-5D	This study
yMM2.10	CEN.PK113-5D	Biosensor	CEN.PK113-5D	This study
	HO::HAA1p-HAA1-mTurquoise2-scENO1t-HREsYGP1p-mCherry-ScSSA1t			
yMM2.11	CEN.PK113-5D	Biosensor	CEN.PK113-5D	This study
	HO::HAA1p-HAA1-mTurquoise2-scENO1t-HREsENO1cp-mCherry-ScSSA1t			
yMM2.12	CEN.PK113-5	Control	CEN.PK113-5D	This study
	HO::HAA1p-BM3R1-HAA1-mTurquoise2-scENO1t-HREsYGP1p-mCherry-ScSSA1t			
yMM3.1	IMX581 HO::HAA1p-BM3R1-HAA1-mTurquoise2-scENO1t-BM3R1_BSsENO1cp-mCherry-ScSSA1t	Acetic acid producer, biosensor	IMX581	This study
yMM3.2	JH18 HO::HAA1p-BM3R1-HAA1-mTurquoise2-scENO1t-BM3R1_BSsENO1cp-mCherry-ScSSA1t	Acetic acid producer, biosensor	JH18	This study
yMM3.3	JH24 HO::HAA1p-BM3R1-HAA1-mTurquoise2-scENO1t-BM3R1_BSsENO1cp-mCherry-ScSSA1t	Acetic acid producer, biosensor	JH24	This study
yMM3.5	JH29 HO::HAA1p-BM3R1-HAA1-mTurquoise2-scENO1t-BM3R1_BSsENO1cp-mCherry-ScSSA1t	Acetic acid producer, biosensor	JH29	This study
yMM3.7	JH37 HO::HAA1p-BM3R1-HAA1-mTurquoise2-scENO1t-BM3R1_BSsENO1cp-mCherry-ScSSA1t	Acetic acid producer, biosensor	JH37	This study

(BM3R1_BSsENO1cp), Haa1-responsive elements followed by the ENO1 core promoter (HREsENO1cp) or the YGP1 promoter enriched with Haa1-responsive elements (HREsYGP1p) were purchased from Biomatik (Kitchener) and named pMM0.8, pMM0.9, pMM0.10 and pMM0.13 (sequences of new parts listed in Table S1, Supporting Information). New level-0 genetic parts containing the HAA1 promoter (HAA1p), the HAA1 ORF, the YGP1 promoter (YGP1p), HAA1-*mTurquoise2* or *mCherry* were obtained through PCR amplification using genomic DNA from *S. cerevisiae* or plasmids MM2.4 and pMitoLOC (Vowinckel et al. 2015; Addgene #58980) as templates, resulting in vectors pMM0.1, pMM0.2, pMM0.6, pMM0.11 and pMM0.12. In the genetic fragment encoding for the fusion protein Haa1-*mTurquoise2*, the HAA1 stop codon (TGA) was replaced by the dinucleotide GG forming, together with *mTurquoise2* upstream adaptor sequence (TATG), a Gly-Met bridge between the two proteins.

In HREsYGP1p, 10 additional Haa1-responsive elements (HREs) were introduced into YGP1p. YGP1p was chosen based on earlier work demonstrating this promoter to be pH responsive (Rajkumar et al. 2016) and dependent on HAA1 expression (Mira, Becker and Sá-Correia 2010a). The five new HREs (e.g. GGC-GAGGGG, the most effective HRE sequence tested *in vivo* by Mira et al. 2011) were designed to replace putative BSs of TFs other than Haa1. TFs targeting YGP1p were found through the *Saccharomyces* Genome Database (Cherry et al. 1998), whereas their binding motives were selected using the YeTFaSCo database (De Boer and Hughes 2012). BM3R1_BSsENO1cp was designed according to Rantasalo et al. (2018) where eight BM3R1 BSs separated by short spacers placed immediately upstream the ENO1 core promoter (ENO1cp) were shown to lead to highest reporter activation among several combinations tested. In HREsENO1cp, the eight BM3R1 BSs were substituted with HREs. Bm3R1 was chosen based on work of Rantasalo et al. (2018), describing BM3R1 being the strongest among six synthetic activators tested in *S. cerevisiae*.

The synthetic transcription factor (sTF) BM3R1-Haa1-*mTurquoise2* was constructed by fusing the N- and C-termini of HAA1 with BM3R1 and *mTurquoise2*, respectively. BM3R1 is a bacterial DNA-binding protein belonging to the TetR family (Ramos et al. 2005), which has been used for development of synthetic activators in yeast (Rantasalo et al. 2018).

Yeast strains were transformed as previously described by Gietz (2014). The genetic constructs were integrated using the CRISPR/Cas9 technology and plasmid EC2.5 (Cámara, Lenitz and Nygård 2020), containing *cas9* and a cassette for expression of the sgRNA. After digestion with NotI, the integration fragment from level 1 (pMM1.11, pMM1.12, pMM1.13, pMM1.15, pMM1.17 harboring either TF or reporter control cassettes) or level 2 MoClo constructs (pMM2.4, pMM2.9, pMM2.10, pMM2.11, pMM2.12, harboring both TF and reporter cassettes) was co-transformed with the Bpil-digested pEC2.5 and annealed oligonucleotides encoding for sgRNA targeting the HO locus (CCAAAGGCA-C AATTTTACGT), flanked by 40-bp sequences for *in vivo* homologous recombination with the sgRNA expression cassette of pEC2.5, resulting in strains yMM1.11, yMM1.12, yMM1.13, yMM1.15, yMM1.17, yMM2.4, yMM2.9, yMM2.10, yMM2.11 and yMM2.12, depicted in Fig. 1.

The control strain mRuby2+ containing the *mRuby2* reporter directly fused to the C-termini of RPL13A encoding a ribosomal protein was constructed using the CRISPR/Cas9 technology, transforming a cut EC2.5 vector (Cámara, Lenitz and Nygård 2020) with an sgRNA targeting the RPL13A locus (GAAG GAAATACAAAATTG) and a dDNA containing the *mRuby2* ORF

amplified from pYTK034 (Addgene #65141) using primers with 40-bp sequences for *in vivo* homologous recombination.

During strain generation, yeast strains were cultivated in YPD medium (20 g L⁻¹ bacterial peptone, 10 g L⁻¹ yeast extract, 20 g L⁻¹ glucose) or in SD medium lacking uracil (0.77 g L⁻¹ CSM without uracil, 6.9 g L⁻¹ YNB w/o AA, 20 g L⁻¹ glucose).

Fluorescence measurements and microscopy

Red fluorescence was measured from cultures grown in 96-well plates in the BioLector, through the mCherry/RFP filter (excitation 580 nm, emission 610 nm, gain 100). The fluorescence values were normalized against the biomass of the cultures, measured as scattered light (excitation 620 nm, emission 620 nm, gain 10). The fold of activation was calculated as the ratio between the fluorescence at a given acetic acid concentration and the fluorescence measured in cultures lacking acetic acid. Data presented are the average of three biological replicates; significant differences between strains were calculated using the two-tailed two-sample unpaired t-test.

For microscopic imaging of Haa1 localization inside the cells upon exposure to different acids, shake flasks were inoculated from precultures to an OD₆₀₀ of 0.1, after which the cultures were incubated shaking at 200 rpm, at 30°C until they reached an OD₆₀₀ of 1. The cultures were subjected to different weak acid stress by adding acetic, lactic, propionic, formic, muconic, glycolic, benzoic or adipic acid stock solution to final concentrations ranging from 500 to 950 mM (for lactic acid) or from 10 to 150 mM for the other acids. The acid-exposed cultures were incubated shaking at 30°C and 1 mL samples were collected immediately, after 5 and after 30 min of incubation. The cells were visualized on an inverted Leica DMI 4000 B fluorescence microscope (Leica Microsystems, Wetzlar, Germany) equipped with a 100× objective.

For visualizing nuclei in cultures exposed to acetic acid, the harvested cells were resuspended in 1 mL of Phosphate Buffered Saline (PBS) solution with 800 ng mL⁻¹ 4',6-diamidino-2-phenylindole (DAPI) and 50 mM acetic acid. The stained cells were incubated at room temperature for 5 min, gently shaking sheltered from light and resuspended in PBS solution with 50 mM acetic acid before being visualized. The filter sets used for all cultures were excitation 436/20 nm, emission 480/40 nm for *mTurquoise2* and excitation 387/11 nm, emission 447/60 nm for DAPI. The collected data were analyzed using the ImageJ software.

Acetic acid measurements

High-performance liquid chromatography (HPLC) was used to measure acetic acid and glucose concentrations of culture samples. The 20 mL of sample was harvested after 21 h of incubation in shake flasks, samples were centrifuged at 3000 rpm, 4°C for 10 min, diluted with MilliQ water and filtered before being measured using a Jasco UV-RI HPLC (LC-4000 series, Tokyo, Japan) equipped with an AS-4150 auto-sampler, a CO-4061 column, a RI-4031 RI detector and a UV-4075 UV detector. Extraction of intracellular metabolites was done as described by Ilmén et al. (2013). In brief, the cell pellet was washed in 20 mL of ice cold 1 M Tris-HCl solution at pH 9.0 and resuspended in 10 mL of ice cold 5% (w/v) trichloroacetic acid (TCA) solution. Cells in TCA were vortexed for 1 min, incubated on ice for 30 min, vortexed again for 1 min and centrifuged at 5500 rpm for 30 min at 4°C. After this, the supernatant was collected, diluted and filtered

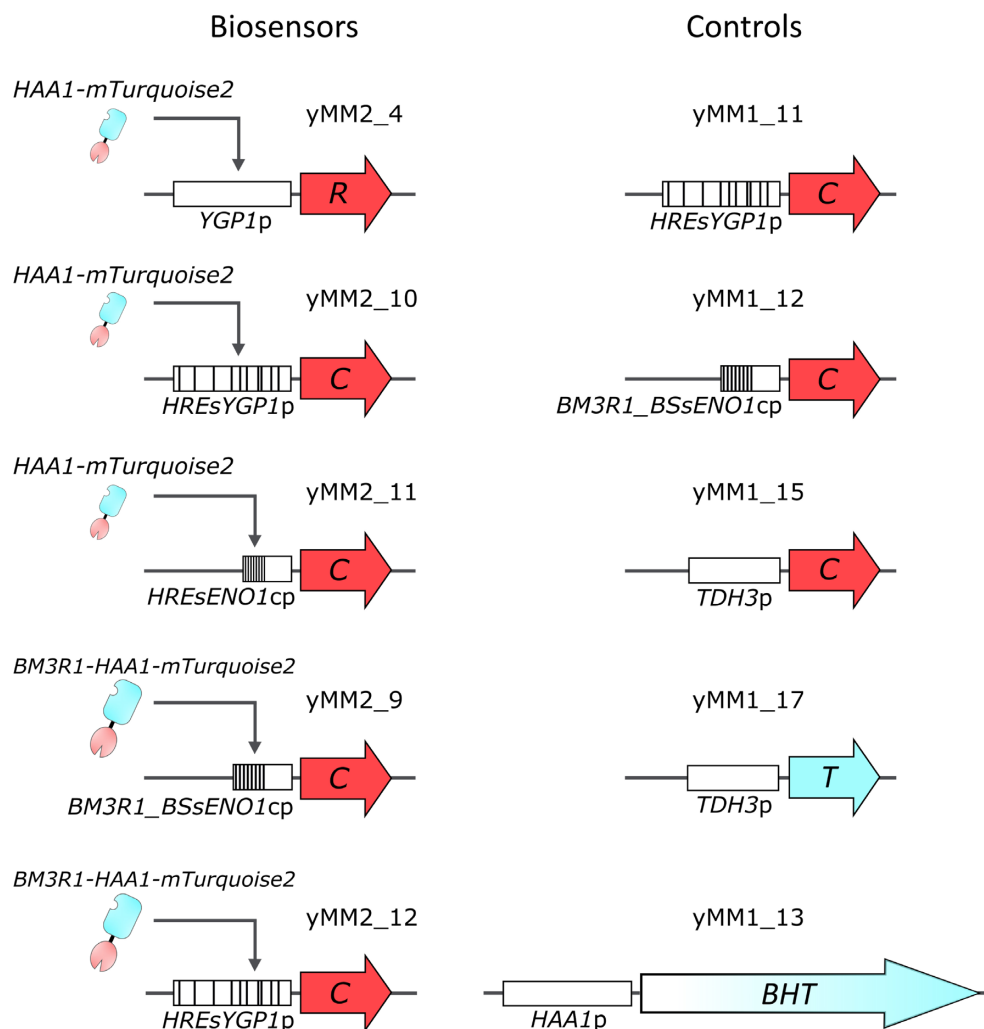


Figure 1. Schematic presentation of the biosensor and control constructs. For strain details, see Table 1. Haa1 with fusion proteins is expected to relocate to the nucleus upon acetic acid exposure. The biosensor output is the expression of the reporter (*mRuby2* or *mCherry*), expressed under various synthetic promoters. Sizes of promoters and genes are scaled to represent their actual sizes and added BSs for the sTFs are indicated with black bars inside the promoters. Red arrows labeled with R and C refer to the *mRuby2* or *mCherry* reporter genes. Cyan arrows labeled with T and BHT refer to *mTurquoise2* or *BM3R1-HAA1-mTurquoise2*.

before HPLC measurement. Compounds were separated using 5 mM H_2SO_4 aqueous solution with a flow rate of 0.8 mL min^{-1} at 80°C. The intracellular concentration of acetic acid was normalized against the cell volume. A CASY device (Schärfe System GmbH, Reutlingen, Germany) was used to assess cell volume and the number of cells in the culture. Five microliters of culture sample was diluted in 10 mL of CASY ton buffer solution (Roche Innovatis, Bielefeld, Germany) and three measurements were performed on each sample. Data were analyzed using the CromNAV software.

RESULTS

Utilizing Haa1 as a biosensor

To investigate the potential of Haa1 as a biosensor, Haa1 was fused to *mTurquoise2* and expressed under the native *HAA1* promoter. As a reporter for Haa1-regulated transcription, *mRuby2* was expressed under the *YGP1* promoter. These constructs were integrated in *S. cerevisiae* yMM2.4 (Table 1; Fig. 1) and the fluorescence of yMM2.4 cells exposed to various acids was studied using fluorescence microscopy. Upon exposure to 50 mM acetic

acid, Haa1-*mTurquoise2* clearly localized to the nucleus of the cells after 30 min (Fig. 2; Table 2). Similarly, cells exposed to lactic, glycolic or muconic acid displayed a clear nuclear localization of Haa1-*mTurquoise2*, while we could not detect nuclear localization of cells exposed to propionic, formic, benzoic or adipic acid (Table 2; Fig. S1, Supporting Information). However, after 30 min of exposure no red fluorescence from the reporter could be detected by fluorescence microscopy of the yMM2.4 cells exposed to different acids (data not shown). After yMM2.4 was cultivated for 18 h in medium with and without 50 mM acetic acid, a 2-fold expression of *mRuby2* was measured for cells exposed to acetic acid compared with cells grown in standard SD medium (Fig. S2, Supporting Information). The expression of the biosensor did not impact the growth of the strain (Fig. S3A, Supporting Information).

Development of a synthetic acetic acid-responsive biosensor

One of the main parameters to consider for the applicability of a biosensor for screening and selection is the dynamic range describing the biosensor's output. For this reason, the

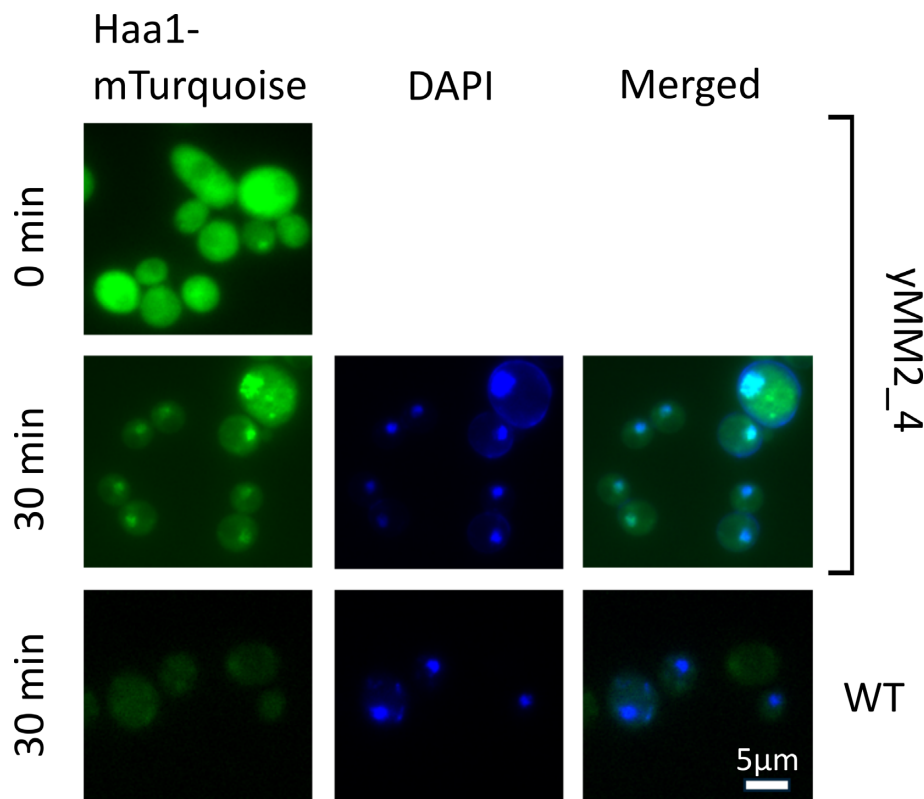


Figure 2. Microscopy pictures of yMM2.4 expressing HAA1-*mTurquoise2* and the parental strain (WT) after exposure to 50 mM acetic acid (pH 5.5) for 0 and 30 min (green). After 30 min of incubation, cells were stained with DAPI (blue) and reimaged.

Table 2. Summary of microscopic studies focusing on localization of Haa1-*mTurquoise2* in yMM2.4 cells upon exposure to different weak acids.

Acid	Chain length	Nuclear localization of Haa1- <i>mTurquoise2</i> ^a	Concentration (mM) ^b	Exposure time (min) ^b
Acetic acid	C2	+	50	30
Lactic acid	C3	+	830	5
Propionic acid	C3		10–150	0, 5, 30
Formic acid	C1		10–150	0, 5, 30
Muconic acid	C6	+	100	30
Glycolic acid	C2	+	50	30
Benzoic acid	C6		10–150	0, 5, 30
Adipic acid	C6		10–150	0, 5, 30

^aThe nuclear localization of Haa1-*mTurquoise2* after reported acid exposure time is indicated with a plus (+) sign.

^bThe acid concentration resulting in Haa1-*mTurquoise2* nuclear localization or the range of concentrations tested for that acid after the indicated exposure time; 10, 25, 50, 100 and 150 mM of propionic, formic, benzoic and adipic acids was tested.

Haa1-based biosensor was developed further (Table 1; Fig. 1). In the new designs, mRuby2 was changed to mCherry, which has been shown to be more stable in low pH, compared with mRuby2 (Shinoda, Shannon and Nagai 2018). As previously published TF-based biosensors have been designed by adding multiple repeats of the TF BSs in the reporter-driving promoter, YGP1p was modified to include 10 additional HREs in yMM2.10. In yMM2.11, YGP1p was substituted with a synthetic promoter, containing eight HREs and the ENO1cp, inspired by the synthetic expression systems described by Rantasalo et al. (2018). In yMM2.9, the TF BM3R1 from *Bacillus megaterium* (Ramos et al. 2005) was fused to the N-terminus of Haa1-*mTurquoise2*, while eight BM3R1 BSs were added upstream the ENO1cp.

A set of controls was designed to ensure the function of the new biosensors. To verify that the expression of the

reporter was dependent on Haa1, BM3R1-*mTurquoise2* expressed under the HAA1 promoter was integrated in yMM1.13 (Table 1; Fig. 1). To determine to what extent the sTF containing both BM3R1 and Haa1 was able to activate a promoter containing HREs, yMM2.12 expressing BM3R1-HAA1-*mTurquoise2* and *mCherry* under the YGP1 promoter containing additional HREs (HREsYGP1p) was used. To assess the level of reporter activation by the endogenous Haa1 (lacking the sTF containing a Haa1 fusion protein), strains expressing the HREsYGP1p-*mCherry* and BM3R1.BSsENO1cp-*mCherry* reporter constructs, but no sTF, were constructed: yMM1.11 (HREsYGP1p-*mCherry*) and yMM1.12 (BM3R1.BSsENO1cp-*mCherry*). In addition, strains expressing *mCherry* (yMM1.15) or *mTurquoise2* (yMM1.17) under the strong, constitutive TDH3 promoter were used as positive controls for the fluorescence measurements.

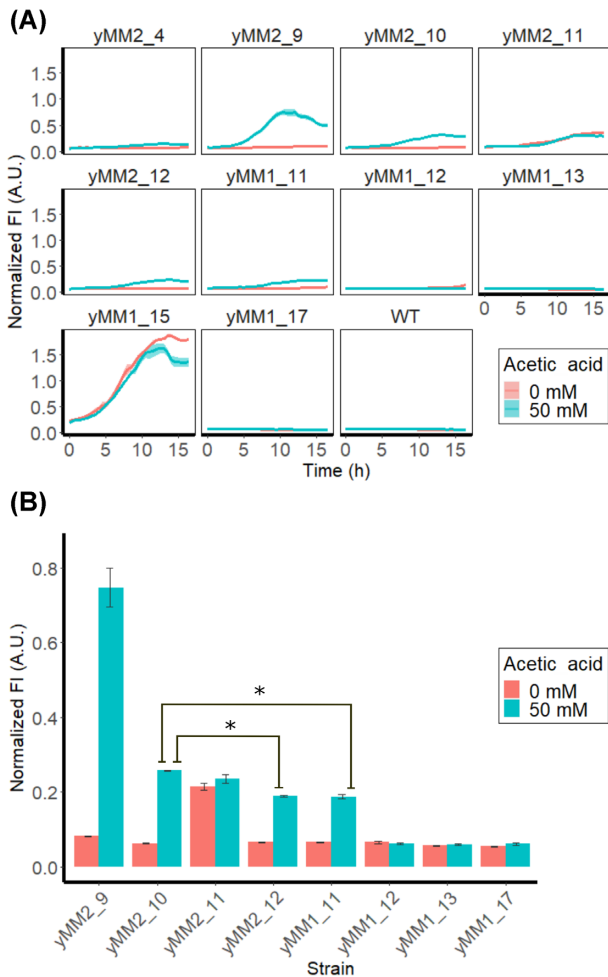


Figure 3. Normalized fluorescence intensity (FI) of the biosensor reporter over time (A) and after 10.5 h of cultivation (B) of strains harboring different biosensors or control constructs, in the absence (in red) and presence (in blue) of 50 mM acetic acid. Cells were cultivated at pH 5.5. Data obtained from three biological replicates, shadowed regions or whiskers show the standard deviation. Statistical significance is represented as “*” for $P \leq 0.001$.

The fluorescence and growth of yeast strains expressing the new biosensors, or the control constructs were monitored in SD medium and SD medium supplemented with 50 mM acetic acid (Fig. 3A). Biosensors of yMM2.4, yMM2.9 and yMM2.10 showed increased reporter expression upon acetic acid exposure compared with their acetic acid-free cultures, reaching a peak in reporter expression after ~10.5 h. The biosensor of yMM2.11 showed equal reporter expression both in presence and absence of acetic acid, with the mCherry signals peaking after ~13 h of cultivation. The parental (WT) or control strains yMM1.12 (BM3R1_BSsENO1cp-mCherry), yMM1.13 (HAA1-mTurquoise2) and yMM1.17 (TDH3p-mTurquoise2) did not show any reporter expression. The positive control yMM1.15 (TDH3p-mCherry) displayed constitutive mCherry expression both in absence and presence of acetic acid. The controls strains yMM1.11 (HREsYGP1p-mCherry) and yMM2.12 (BM3R1-HAA1-mTurquoise2...HREsYGP1p-mCherry) showed increased reporter expression upon acetic acid induction, peaking after ~13.5 h of cultivation.

The reporter expression of the control strains yMM1.11 (HREsYGP1p-mCherry) and yMM2.12 (BM3R1-HAA1-mTurquoise2...HREsYGP1p-mCherry) was similar ($P = 0.36$ after 10.5 h of cultivation), suggesting that the presence of

the sTF BM3R1-Haa1-mTurquoise2 had no impact on the reporter expression when mCherry was expressed under the control of the YGP1 promoter containing additional HREs (Fig. 3B). On the contrary, yMM2.10 and yMM2.12 (both containing the HREsYGP1p-mCherry reporter but co-expressing HAA1-mTurquoise2 or BM3R1-HAA1-mTurquoise2) displayed a significantly different reporter expression upon acetic acid exposure ($P < 0.001$ after 10.5 h of cultivation), the expression of yMM2.10 being ~1.4-fold higher than yMM2.12 (Fig. 3B). The biosensor of yMM2.11 gave highest basal reporter expression that was merely 1.1-fold increased upon acetic acid exposure. The biosensor of yMM2.10 (Haa1-mTurquoise2 TF with HREsYGP1p-mCherry reporter) showed ~4-fold increase in fluorescence upon acetic acid exposure. Strain yMM2.9, harboring the biosensor containing the BM3R1-Haa1-mTurquoise2 sTF and the BM3R1_BSsENO1cp-mCherry reporter, displayed the best dynamic range, as determined by level of induction in the presence of acetic acid. The acetic acid-induced reporter expression of the biosensor of yMM2.9 was the strongest among all biosensors, both in terms of absolute fluorescence value and relative induction (~9-fold expression of mCherry compared with the basal expression). Therefore, the biosensor of yMM2.9 was selected for further investigations. The expression of the biosensor did not impact the growth of the strain (Fig. S3B, Supporting information).

Characterization of the acetic acid biosensor

The biosensor expressed in yMM2.9 was characterized at different growth conditions. Reporter expression and growth were monitored over time at different pH and at different acetic acid concentrations (Fig. 4A and B; Fig. S4, Supporting Information). The biosensor gave the highest reporter signal, both in absolute terms and in relation to the basal expression in medium lacking acetic acid, when yMM2.9 was grown at a pH of 4 or 3.5 (Fig. 4A). The biosensor induction at pH 3.5 or 4 was ~6.5-fold compared with the basal expression. The fluorescence of yMM2.9 exposed to acetic acid was at pH 4.5 ~96% of the maximal fluorescence measured at pH 3.5 or 4, but it also registered a higher basal activity, resulting in an acetic acid-dependent induction of ~5.7-fold. At pH 4.5 and 5 the fluorescence of the biosensor reporter was ~63% and 34% of the maximal fluorescence, respectively (Fig. 4A). Cells cultivated at pH 2.5 grew very poorly, even in the absence of acetic acid, and the fluorescence signal at pH 2.5 in presence of 50 mM acetic acid was below the background signal (Fig. S4, Supporting Information). The normalized fluorescence of yMM2.9 growing in medium lacking acetic acid was similar at pH 3.5–5 and slightly higher at pH 3, where strain growth was also impaired (Fig. 4A; Fig. S4, Supporting Information).

yMM2.9 cells cultivated in the presence of 10–60 mM of acetic acid displayed a linear increase in the reporter signal when exposed to increasing concentration of acetic acid (Fig. 4B and C). At 60–80 mM acetic acid cells showed increased lag phases and delayed reporter expression, and at 90–100 mM acetic acid cells did not grow (Fig. 4B; Fig. S4D, Supporting Information). Cells grown in 70 mM acetic acid displayed highest reporter expression after 25 h of cultivation, when the expression was similar to that of the culture at 60 mM (Fig. S4, Supporting Information).

In order to further characterize the biosensor, acetic acid was added to cultures of yMM2.9 at different time points; at the start of the cultivation, after 5 or 10 h of cultivations when the cells were growing exponentially, after 24 h when cells were past the

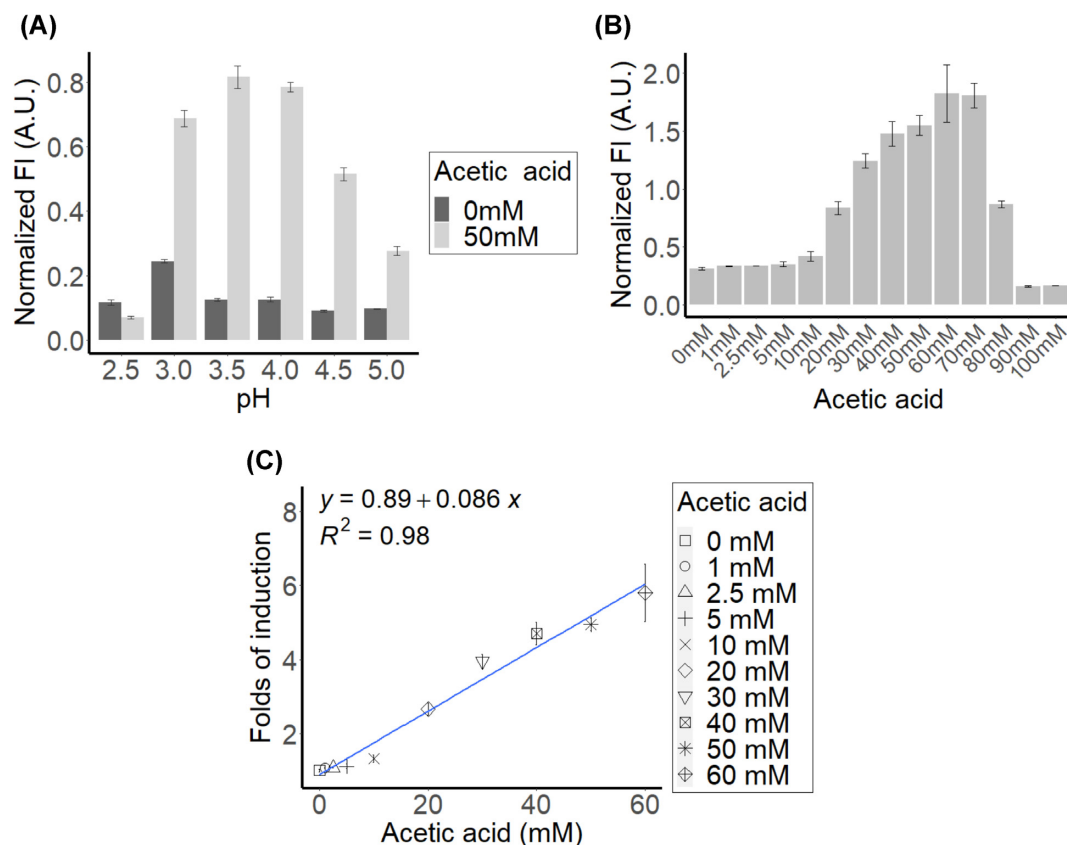


Figure 4. Normalized FI of yMM2.9 at (A) different pH or (B) in the presence of varying amounts of acetic acid, at pH 3.5. FI value presents the highest value measure for each condition. (C) The fold of induction of the biosensor in presence of varying concentrations of acetic acid plotted against the acetic acid concentration used. Fold of inductions represents the ratio between the fluorescence of yMM2.9 at a given acetic acid concentration compared with its basal fluorescence in medium lacking acetic acid. The linear regression of the data is shown with a blue line and the Pearson correlation coefficient (R^2) is indicated in the plot. The fluorescence values represent the maximum normalized FI observed for each condition. Data obtained from three biological replicates; whiskers show the standard deviation.

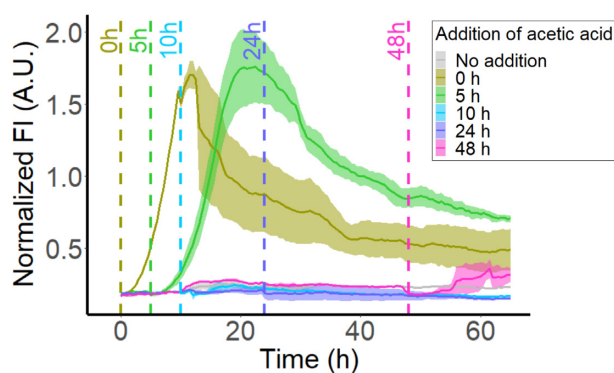


Figure 5. Biosensor output upon acetic acid addition to the cultures at different time points. Normalized FI of the reporter in yMM2.9 cells with acetic acid injected at different time points (dashed lines) to a final concentration of 50 mM, pH 3.5. Data obtained from three biological replicates; shadowed regions show the standard deviation.

diauxic shift or after 48 h when the cells had reached the stationary phase (Fig. S5, Supporting Information). When acetic acid was added in the beginning of the cultures or after 5 h of cultivation, the fluorescence of the cultures rapidly increased, reaching its peak ~10 h later (Fig. 5). Nonetheless, when the acetic acid was added to the cultures at later time points, no increase in fluorescence was measured.

Applying the biosensor for measuring acetic acid production

In order to use the biosensor for measuring acetic acid produced by yeast, the characterized biosensor (pMM2.9) was integrated into a set of strains engineered to produce acetyl-CoA derived products (Hellgren *et al.* 2020). These strains, originally engineered to produce 3-hydroxypropionic acid, express a generalist phosphoketolase encoding gene (Xfspk) enabling non-oxidative glycolysis (Hellgren *et al.* 2020) and contain other modifications leading to different amounts of acetic acid being produced (Fig. 6; Fig. S7, Supporting Information). The acetic acid-producing cells harboring the biosensor (yMM3.1, yMM3.2, yMM3.3, yMM3.5, yMM3.7; Table 2) were cultivated in shake flasks and their extra- and intracellular acetic acid production, as well as glucose consumption and biosensor reporter expression, was measured after 21 h of growth. The highest acetic acid titer was measured for yMM3.5 (1.7 g L⁻¹), followed by yMM3.3 (1.3 g L⁻¹), yMM3.7 (1.1 g L⁻¹), yMM3.2 (0.9 g L⁻¹) and yMM3.1 (0 g L⁻¹) (Fig. 6B). The intracellular acetic acid concentration was normalized by the estimated cell volume; yMM3.3 displayed the highest intracellular acetic acid concentration (11.7 g L⁻¹), followed by yMM3.2 (9 g L⁻¹), yMM3.7 (8.4 g L⁻¹), yMM3.5 (7.3 g L⁻¹) and yMM3.1 (1.6 g L⁻¹) (see Fig. 6C). After 21 h of growth, the glucose was completely depleted in all acetic acid-producing cultures, except for yMM3.5 that had 1.1 g L⁻¹ glucose left in the medium (Fig. 6D). The biosensor reporter fluorescence showed a

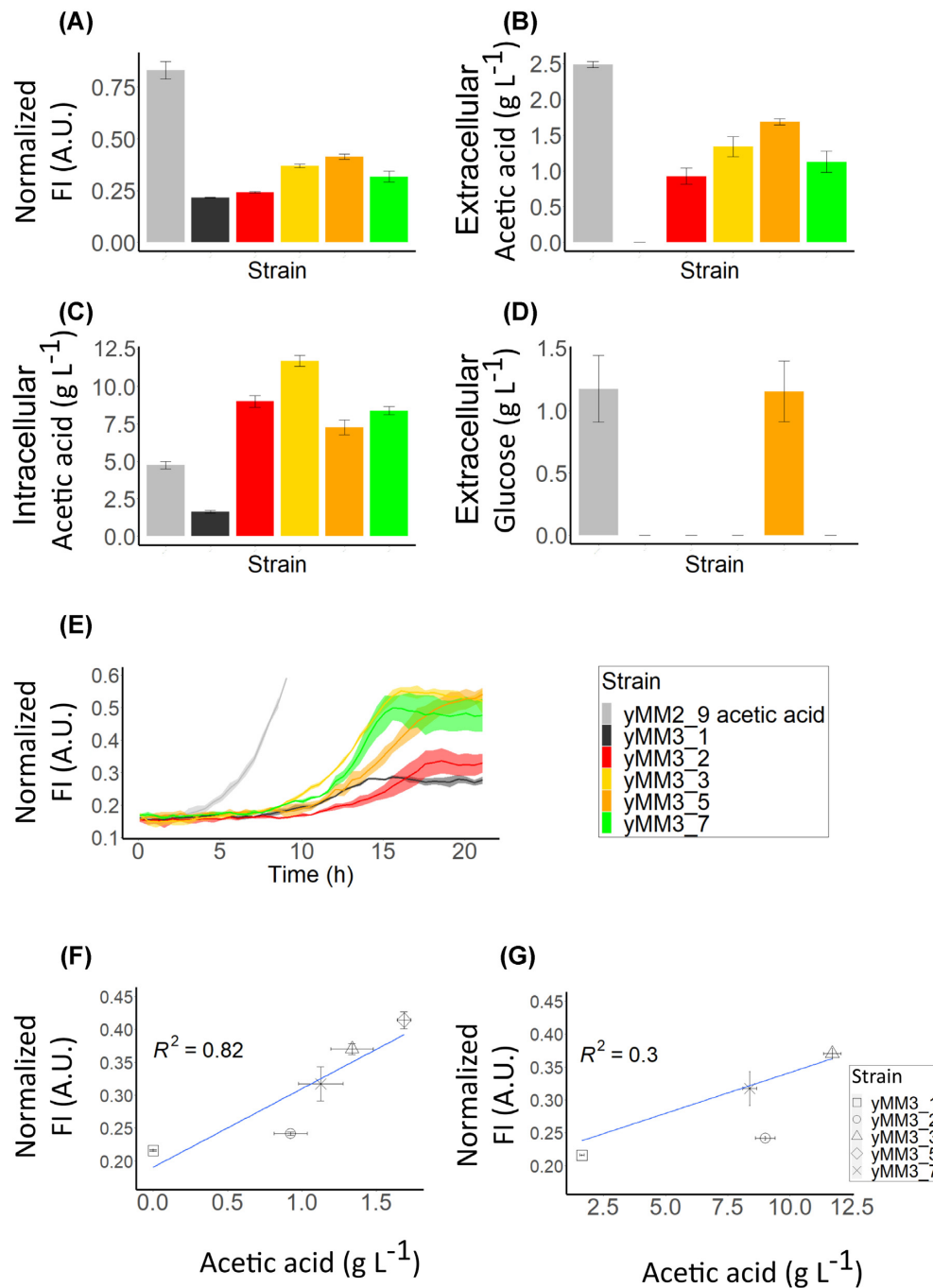


Figure 6. Normalized FI (A), extracellular acetic acid (B), intracellular acetic acid (C) and extracellular glucose (D) concentrations after 21 h of cultivation of the biosensor strain grown in SD medium at pH 3.5, with 50 mM acetic acid (yMM2.9 acetic acid) and the acetic acid-producing strains with a biosensor grown in SD medium at pH 3.5 (yMM3.1,2,3,5&7). (E) Normalized FI measured over time for the cultivations. Scatterplot displaying the extracellular (F) or intracellular (G) acetic acid concentrations against the normalized FI of the cultures. The linear regression of the data is shown with a blue line and the Pearson correlation coefficient (R^2) is indicated in the plots. Data obtained from three biological replicates; shadowed regions show the standard deviation.

high correlation ($R^2 = 0.82$) to the acetic acid titer of the strains (Fig. 6A, E and F): the highest reporter signal was measured for yMM3.5, followed by yMM3.3, yMM3.7, yMM3.2 and yMM3.1. In contrast, no clear correlation ($R^2 = 0.3$) was observed between the biosensor output and the intracellular acetic acid concentration measured from cells collected at 21 h (Fig. 6G).

The biosensor reporter signal and growth of the acetic acid-producing strains were also monitored over time (Fig. 6E; Fig. S6, Supporting Information). After 21 h of cultivation, strains

yMM3.3 and yMM3.5 displayed the highest fluorescent reporter expression, followed by yMM3.7, yMM3.2 and yMM3.1. Furthermore, the biosensor output began to increase at different times depending on the strain, for yMM3.3 and yMM3.7 after ~ 8 h of cultivation, followed by yMM3.1 and yMM3.5 after ~ 10 h and yMM3.2 after ~ 12 h. The strain producing the lowest amount of acetic acid, yMM3.1, started to grow after ~ 5 h of cultivation, whereas the lag phase was ~ 7 h for the other strains (Fig. S6, Supporting Information).

DISCUSSION

Ligand-binding TFs have been widely used for the construction of biosensors that can be used to detect and monitor molecules of interest. TF-based biosensors have been used for screening strain libraries producing a specific compound, or for detecting a specific environmental condition or even as parts of regulatory pathways. In this study, we engineered the native *S. cerevisiae* TF Haa1 to be used as a biosensor for detecting acetic acid. Haa1 localizes to the nucleus upon binding of acetic acid (Collins, Black and Liu 2017), and by coupling this TF to the prokaryotic repressor BM3R1 (Ramos et al. 2005), we constructed a molecular device capable to detect and report acetic acid production and concentration in the culture.

Synthetic TFs containing prokaryotic repressor elements are well established in *S. cerevisiae* (Mojzita, Rantasalo and Jäntti 2019). Such TFs have been used for various orthogonal expression systems (Mojzita, Rantasalo and Jäntti 2019) and also as parts of biosensors (Qiu, Zhai and Hou 2019). The sTFs drive expression of genes, often under the control of synthetic promoters containing a core promoter and a set of BSs for the TF. Core promoters are short promoter sequences, serving as binding platform for the transcription machinery, that on their own can drive expression of genes but generally with (very) low basal activity (Haberle and Stark 2018). When a core promoter is fused to a sequence containing BSs for a specific TF, this can lead to expression of different strength, depending on the core promoter used and number of BSs present in the synthetic promoter (Rantasalo et al. 2018; Mózsik et al. 2019). Based on experiences by Rantasalo et al. (2018), we chose to fuse the bacterial DNA-binding protein BM3R1 to Haa1 and use a synthetic promoter containing the ENO1cp and BSs for BM3R1 for driving the expression of the reporter, mCherry. The fusion of Haa1 to BM3R1 was needed as the mCherry fluorescence of yMM2.11 containing HAA1-mTurquoise2 and the synthetic promoter with eight HREs (instead of the BM3R1 BSs) was shown not to be induced by acetic acid. The mCherry expression of yMM2.11 was strong already at basal conditions (Fig. 3A), which may explain why no increase in expression was seen when the cells were grown in the presence of 50 mM acetic acid.

Many factors including the biosensor design, cultivation media and physical growth parameters influence biosensor performance. Our biosensor was built around the endogenous TF Haa1 that regulates acid tolerance (Mira, Teixeira and Sá-Correia 2010b; Sugiyama et al. 2014) and when overexpressed is known to give a fitness benefit in medium with acetic acid (Tanaka et al. 2012; Swinnen et al. 2017). Therefore, we constructed a set of controls for ensuring the orthogonality of the biosensor (Fig. 1). The mCherry fluorescence measured from yMM1.11 and yMM2.12, both bearing a construct with the YGP1 promoter engineered to contain additional HREs, was similar even though yMM2.12 also expressed the sTF of the biosensor (Figs 1 and 3B). In contrast, in yMM2.10 where Haa1-mTurquoise2 regulated the expression of mCherry under a synthetic promoter containing HREs, the reporter signal was significantly higher in the presence of acetic acid, both in terms of absolute fluorescence ($P < 0.001$ compared with strain yMM1.11 bearing only the synthetic promoter driving mCherry) and fold of induction (4-fold increase for yMM2.10 versus 3-fold increase for yMM1.11, compared with their respective basal conditions). This indicated that, unlike Haa1-mTurquoise2, the sTF BM3R1-Haa1-mTurquoise2 could not regulate the expression of genes under the control of a promoter containing HREs. Thus, the biosensor

constructed should not interfere with the endogenous Haa1 regulatory network. In line with this, the expression of the biosensor did not impact growth of the cells exposed to acetic acid (Fig. S3, Supporting Information). Therefore, we concluded that an additional copy of HAA1 as part of the biosensor or the biosensor itself did not have any noticeable effect on the physiology of the cells.

In order to use a biosensor, its features such as specificity, sensitivity and dynamic range need to be characterized. The biosensor designed in this study was expectedly shown to have weak specificity, as Haa1 was known to bind both acetic and lactic acids (Sugiyama et al. 2014; Collins, Black and Liu 2017), and activate target genes under stress caused by propionic, sorbic and benzoic acids (Kim et al. 2018). Indeed, nuclear localization of Haa1 was observed upon exposure to acetic, lactic, glycolic or muconic acid (Fig. 2; Table 2; Fig. S1, Supporting Information). Consistent with previous studies (Kim et al. 2018), describing that the degree of activation by Haa1 varies depending on which acid the cells are exposed to, we could not see any clear nuclear localization of Haa1 in cells exposed to propionic, formic, benzoic or adipic acid (Table 2). Nonetheless, as Kim et al. (2018) reported activation of Haa1 target genes in cells exposed to propionic or benzoic acid, it is still likely that Haa1 can also bind these acids. In fact, the promiscuity of Haa1 represents an opportunity for expanding the application of the biosensor developed to other acids produced by the cells. Lactic, muconic and glycolic acids are all potential platform chemicals used for the production of biopolymers. Recently, a muconic acid biosensor based on a prokaryotic TF was used to screen mutant libraries of muconic acid-producing yeast (Wang et al. 2020), demonstrating the potential for biosensor-based screening of production strains.

To further characterize the biosensor, we analyzed its dynamic and operational range. The biosensor's mCherry reporter was expressed up to 6-fold upon acetic acid presence compared with expression in basal medium (Fig. 4C). This relatively low dynamic range is in line with what previous studies describing biosensors in yeast (Li et al. 2015; Liu et al. 2017; Dabirian et al. 2019) have reported. The operational range of the biosensor was shown to span 10–60 mM acetic acid (0.6–3.6 g L⁻¹; Fig. 4B; Fig. S4C and D, Supporting Information). Nonetheless, as the growth of *S. cerevisiae* was severely impaired at higher concentrations of acetic acid (Fig. S4B, Supporting Information), the operational range of our biosensor was limited by the strains' tolerance to acetic acid, which is highly dependent on the pH of the medium. Still, biosensors with similar or smaller operational ranges have successfully been used for FACS-based screens (Li et al. 2015; Dabirian et al. 2019; Hahne, Rödel and Ostermann 2021) and synthetic control circuits (Wang, Barahona and Buck 2013; Wu et al. 2020). Previous studies demonstrated that an increased dynamic range of an expression system can be achieved by tuning the expression of the sTF and the number of TF BSs in the promoter driving the reporter (Rantasalo et al. 2016; Mózsik et al. 2019) or mutagenesis of the sTF (Jester et al. 2018). Moreover, mutagenesis has been reported as a successful method for increasing biosensor specificity (Feng et al. 2015; Skjoedt et al. 2016; Jester et al. 2018). Similar approaches may be taken to optimize the dynamic and operational range of the acetic acid biosensor developed here.

In a recent study, expression of a fluorescent protein under the YGP1 promoter was used to monitor acetic acid in the extracellular medium of *S. cerevisiae* (Hahne, Rödel and Ostermann 2021). In the study by Hahne, Rödel and Ostermann (2021), up to

30 mM of acetic acid could be detected by their biosensor strain that was applied for detecting acetic acid in biogas production. The use of ligand-binding, TF-based biosensors may provide greater specificity and orthogonality compared with the use of native stress-responsive promoters as biosensors (Mojzita, Rantasalo and Jäntti 2019). Thus, another application for the biosensor we constructed could be its use as a whole-cell biosensor for processes where acids are released, such as hydrolysis of biomass that leads to the formation of acetic and formic acids (Klinke 2004).

Here, we used the biosensor to monitor acetic acid production in a set of strains engineered to accumulate relatively high levels of acetic acid (Hellgren et al. 2020). We observed a high correlation ($R^2 = 0.82$) between the mCherry reporter output and the acetic acid produced by the strains, as measured by HPLC (Fig. 6F). Instead, no correlation ($R^2 = 0.3$) was observed between the reporter output and the intracellular acetic acid measured (Fig. 6G). Here, the two outliers yMM3.2 and yMM3.5 displayed significantly higher and lower acetic acid concentrations compared with the trendline. This could be due to glucose-repressed cells being less permeable to acetic acid anions (Cassio, Leao and Van Uden 1987), leading to more acetic acid being captured and accumulated intracellularly when glucose is not present in the medium. This would explain the lower intracellular acetic acid concentrations measured in yMM3.5 cells, as there was still glucose present in the medium of the yMM3.5 cultures after 21 h when the intracellular acetic acid was measured (Fig. 6C). Similarly, as yMM3.2 grew faster than the other strains that produced high amounts of acetic acid (Fig. S6, Supporting Information), it likely rapidly depleted the glucose of the medium and therefore it may be that the yMM3.2 cells accumulated more intracellular acetic acid than other strains even if the overall production was lower. Furthermore, the acetic acid addition experiments indicated that the time point of exposure was crucial for the biosensor output. Our biosensor was shown to work during cell growth; when acetic acid was injected at the end of the exponential phase or later during the cultivation, no mCherry reporter increment could be measured (Fig. 5; Fig. S5, Supporting Information). By monitoring the biosensor output over time, we saw different starting points for reporter expression, indicating that acetic acid production of the strains started at different time points (Fig. 6E). The reporter signal of yMM3.5 was still increasing at 21 h when the cultivation was stopped, while the reporter signal of the other strains had already reached a plateau at this time point (Fig. 6E). This indicates that acetic acid was still being produced and likely also exported continuously. Cell-to-cell heterogeneity in cells used for acid production has been reported earlier and high concentrations of intracellular acids have been reported to be detrimental for the cells (Nygård et al. 2014a,b). Thus, single-cell monitoring of acetic acid production and viability of the cells may provide a better understanding for the discrepancy in biosensor output and production seen at the population level.

Extracellular acetic acid can enter the cells through unspecific transport processes or passive diffusion (Casal, Cardoso and Leão 1996), whereas inside the cells at neutral pH, the acetic acid dissociates to protons and acetic acid ions that are unable to diffuse through the plasma membrane and thus accumulate intracellularly (Palma, Guerreiro and Sá-Correia 2018). This means that the intracellular concentration of acetic acid in cells producing acetic acid or exposed to acetic acid is a constant balance where the acid enters the cells, depending on the extracellular pH. The pK_a of acetic acid is 4.76; thus, at pH below 4.76, the acetic acid is mainly in its undissociated form, CH_3COOH ,

which is able to passively cross the cell membrane back into the cells. We noted that even though our biosensor worked at quite a wide pH range (pH 3–5; Fig. 4A), the dynamic range of the biosensor was greatest at pH 3.5–4 (Fig. 4A). This may be due to different binding affinity of the undissociated and dissociated forms of acetic acid or simply due to the higher proportion of dissociated acetic acid that cannot enter the cells at higher pH. At very low pH, on the other hand, the cells are stressed by the presence of acetic acid (Mira, Becker and Sá-Correia 2010a), which leads to poor growth (Fig. S4E and F, Supporting Information) and potentially less energy and resources available for maintaining the biosensor.

In conclusion, with this study we demonstrated the possibility to use the Haa1 TF to create a biosensor capable of measuring acetic acid added to the growth medium or produced by the cells. The biosensor was characterized and used in strains producing different levels of acetic acid. This tool could be used for high-throughput screenings and for monitoring the acetic acid production over time. The biosensor could also be suitable for screening of acetic acid-tolerant strains or optimized for sensing other organic acids. While many previous studies have described biosensors containing prokaryotic ligand-binding TFs, this is to our knowledge the first study where an endogenous ligand-binding TF is used as a biosensor in *S. cerevisiae*. We believe that this work could inspire the development of many more endogenous TF-based biosensors that could be applied toward screening and improving strains to be used for various biorefinery applications.

ACKNOWLEDGMENTS

The authors would like to thank John Hellgren for generously providing them with the acetic acid-producing strains that were used to demonstrate the applicability of the biosensor. Luca Torello Pianale is thanked for providing the mRuby2+ strain. Merja Penttilä and Dominik Mojzita are thanked for fruitful discussions during the project.

SUPPLEMENTARY DATA

Supplementary data are available at *FEMSYR* online.

FUNDING

This work was supported by the Swedish Research Council Formas (Dnr 2017-00979), the Hasselblad Foundation, Ollie och Elof Ericssons Stiftelser and the Adlerbertska Research Foundation.

Conflict of interest. None declared.

REFERENCES

- Bovee TFH, Helsdingen RJR, Hamers ARM et al. A new highly specific and robust yeast androgen bioassay for the detection of agonists and antagonists. *Anal Bioanal Chem* 2007;**389**: 1549–58.
- Cámara E, Lenitz I, Nygård Y. A CRISPR activation and interference toolkit for industrial *Saccharomyces cerevisiae* strain KE6-12. *Sci Rep* 2020;**10**:1–13.
- Casal M, Cardoso H, Leão C. Mechanisms regulating the transport of acetic acid in *Saccharomyces cerevisiae*. *Microbiology* 1996;**142**:1385–90.

- Cassio F, Leao C, Van Uden N. Transport of lactate and other short-chain monocarboxylates in the yeast *Saccharomyces cerevisiae*. *Appl Environ Microbiol* 1987;**53**:509–13.
- Cherry JM, Adler C, Ball C et al. SGD: *Saccharomyces* Genome Database. *Nucleic Acids Res* 1998;**26**:73–9.
- Chou HH, Keasling JD. Programming adaptive control to evolve increased metabolite production. *Nat Commun* 2013;**4**:1–8.
- Collins ME, Black JJ, Liu Z. Casein kinase I isoform Hrr25 is a negative regulator of Haa1 in the weak acid stress response pathway in *Saccharomyces cerevisiae*. *Appl Environ Microbiol* 2017;**83**:1–15.
- Dabirian Y, Gonçalves Teixeira P, Nielsen J et al. FadR-based biosensor-assisted screening for genes enhancing fatty Acyl-CoA pools in *Saccharomyces cerevisiae*. *ACS Synth Biol* 2019;**8**:1788–800.
- De Boer CG, Hughes TR. YeTFaSCo: a database of evaluated yeast transcription factor sequence specificities. *Nucleic Acids Res* 2012;**40**:169–79.
- Dong Y, Hu J, Fan L et al. RNA-Seq-based transcriptomic and metabolomic analysis reveal stress responses and programmed cell death induced by acetic acid in *Saccharomyces cerevisiae*. *Sci Rep* 2017;**7**:1–16.
- Entian KD, Kötter P. 25 Yeast genetic strain and plasmid collections. *Methods Microbiol* 2007;**36**:629–66.
- Feng J, Jester BW, Tinberg CE et al. A general strategy to construct small molecule biosensors in eukaryotes. *eLife* 2015;**4**:1–23.
- Giannattasio S, Guaragnella N, Zdravlević M et al. Molecular mechanisms of *Saccharomyces cerevisiae* stress adaptation and programmed cell death in response to acetic acid. *Front Microbiol* 2013;**4**:33.
- Gietz RD. Yeast transformation by the LiAc/SS carrier DNA/PEG method. *Methods Mol Biol* 2014;**1163**:33–44.
- Guaragnella N, Antonacci L, Passarella S et al. Achievements and perspectives in yeast acetic acid-induced programmed cell death pathways. *Biochem Soc Trans* 2011;**39**:1538–43.
- Guaragnella N, Bettiga M. Acetic acid stress in budding yeast: from molecular mechanisms to applications. *Yeast* 2021;**38**:391–400.
- Haberle V, Stark A. Eukaryotic core promoters and the functional basis of transcription initiation. *Nat Rev Mol Cell Biol* 2018;**19**:621–37.
- Hahne K, Rödel G, Ostermann K. A fluorescence-based yeast sensor for monitoring acetic acid. *Eng Life Sci* 2021;**21**:303–13.
- Hellgren J, Godina A, Nielsen J et al. Promiscuous phosphoketolase and metabolic rewiring enables novel non-oxidative glycolysis in yeast for high-yield production of acetyl-CoA derived products. *Metab Eng* 2020;**62**:150–60.
- Ilmén M, Koivuranta K, Ruohonen L et al. Production of l-lactic acid by the yeast *Candida sonorensis* expressing heterologous bacterial and fungal lactate dehydrogenases. *Microb Cell Fact* 2013;**12**:1–15.
- Jell J, Merali S, Hensen ML et al. Genetically altered expression of spermidine/spermine N1-acetyltransferase affects fat metabolism in mice via acetyl-CoA. *J Biol Chem* 2007;**282**:8404–13.
- Jester BW, Tinberg CE, Rich MS et al. Engineered biosensors from dimeric ligand-binding domains. *ACS Synth Biol* 2018;**7**:2457–67.
- Jeukendrup AE. Regulation of fat metabolism in skeletal muscle. *Ann N Y Acad Sci* 2002;**967**:217–35.
- Kim MS, Cho KH, Park KH et al. Activation of Haa1 and War1 transcription factors by differential binding of weak acid anions in *Saccharomyces cerevisiae*. *Nucleic Acids Res* 2019;**47**:1211–24.
- Klinke MHB. Inhibition of ethanol-producing yeast and bacteria by degradation products produced during pre-treatment of biomass. *Appl Microbiol Biotechnol* 2004;**66**:10–26.
- Lee ME, DeLoache WC, Cervantes B et al. A highly characterized yeast toolkit for modular, multipart assembly. *ACS Synth Biol* 2015;**4**:975–86.
- Li S, Si T, Wang M et al. Development of a synthetic malonyl-CoA sensor in *Saccharomyces cerevisiae* for intracellular metabolite monitoring and genetic screening. *ACS Synth Biol* 2015;**4**:1308–15.
- Liu Y, Zhuang Y, Ding D et al. Biosensor-based evolution and elucidation of a biosynthetic pathway in *Escherichia coli*. *ACS Synth Biol* 2017;**6**:837–48.
- Mans R, van Rossum HM, Wijsman M et al. CRISPR/Cas9: a molecular Swiss army knife for simultaneous introduction of multiple genetic modifications in *Saccharomyces cerevisiae*. *FEMS Yeast Res* 2015;**15**:fov004.
- Mira NP, Becker JD, Sá-Correia I. Genomic expression program involving the Haa1p-regulon in *Saccharomyces cerevisiae* response to acetic acid. *OMICS* 2010a;**14**:587–601.
- Mira NP, Henriques SF, Keller G et al. Identification of a DNA-binding site for the transcription factor Haa1, required for *Saccharomyces cerevisiae* response to acetic acid stress. *Nucleic Acids Res* 2011;**39**:6896–907.
- Mira NP, Teixeira MC, Sá-Correia I. Adaptive response and tolerance to weak acids in *Saccharomyces cerevisiae*: a genome-wide view. *OMICS* 2010b;**14**:525–40.
- Mojzita D, Rantasalo A, Jäntti J. Gene expression engineering in fungi. *Curr Opin Biotechnol* 2019;**59**:141–9.
- Mózsik L, Büttel Z, Bovenberg RAL et al. Synthetic control devices for gene regulation in *Penicillium chrysogenum*. *Microb Cell Fact* 2019;**18**:1–13.
- Mukherjee V, Lind U, St. Onge RP et al. A CRISPRi screen of essential genes reveals that proteasome regulation dictates acetic acid tolerance in *Saccharomyces cerevisiae*. *mSystems* 2021;**6**:e0041821.
- Nygård Y, Maaheimo H, Mojzita D et al. Single cell and *in vivo* analyses elucidate the effect of xylC lactonase during production of D-xylonate in *Saccharomyces cerevisiae*. *Metab Eng* 2014a;**25**:238–47.
- Nygård Y, Mojzita D, Toivari M et al. The diverse role of Pdr12 in resistance to weak organic acids. *Yeast* 2014b;**31**:219–32.
- Palma M, Guerreiro JF, Sá-Correia I. Adaptive response and tolerance to acetic acid in *Saccharomyces cerevisiae* and *Zygosaccharomyces bailii*: a physiological genomics perspective. *Front Microbiol* 2018;**9**:1–16.
- Palmqvist E, Hahn-Hägerdal B. Fermentation of lignocellulosic hydrolysates. II: inhibitors and mechanisms of inhibition. *Bioresour Technol* 2000;**74**:25–33.
- Pampulha ME, Loureiro-Dias MC. Activity of glycolytic enzymes of *Saccharomyces cerevisiae* in the presence of acetic acid. *Appl Microbiol Biotechnol* 1990;**34**:375–80.
- Qiu C, Zhai H, Hou J. Biosensors design in yeast and applications in metabolic engineering. *FEMS Yeast Res* 2019;**19**:foz082.
- Rajkumar AS, Liu G, Bergenholm D et al. Engineering of synthetic, stress-responsive yeast promoters. *Nucleic Acids Res* 2016;**44**:e136.
- Ramos JL, Martínez-Bueno M, Molina-Henares AJ et al. The TetR family of transcriptional repressors. *Microbiol Mol Biol Rev* 2005;**69**:326–56.
- Rantasalo A, Czeizler E, Virtanen R et al. Synthetic transcription amplifier system for orthogonal control of gene expression in *Saccharomyces cerevisiae*. *PLoS One* 2016;**11**:e0148320.

- Rantasalo A, Kuivanen J, Penttilä M et al. Synthetic toolkit for complex genetic circuit engineering in *Saccharomyces cerevisiae*. *ACS Synth Biol* 2018;7:1573–87.
- Robak K, Balcerek M. Review of second generation bioethanol production from residual biomass. *Food Technol Biotechnol* 2018;56:174–87.
- Shinoda H, Shannon M, Nagai T. Fluorescent proteins for investigating biological events in acidic environments. *Int J Mol Sci* 2018;19:1548.
- Skjoedt ML, Snoek T, Kildegaard KR et al. Engineering prokaryotic transcriptional activators as metabolite biosensors in yeast. *Nat Chem Biol* 2016;12:951–8.
- Sugiyama M, Akase SP, Nakanishi R et al. Nuclear localization of Haa1, which is linked to its phosphorylation status, mediates lactic acid tolerance in *Saccharomyces cerevisiae*. *Appl Environ Microbiol* 2014;80:3488–95.
- Swinnen S, Henriques SF, Shrestha R et al. Improvement of yeast tolerance to acetic acid through Haa1 transcription factor engineering: towards the underlying mechanisms. *Microb Cell Fact* 2017;16:1–15.
- Tanaka K, Ishii Y, Ogawa J et al. Enhancement of acetic acid tolerance in *Saccharomyces cerevisiae* by overexpression of the Haa1 gene, encoding a transcriptional activator. *Appl Environ Microbiol* 2012;78:8161–3.
- van Dijk M, Trollmann I, Saraiva MAF et al. Small scale screening of yeast strains enables high-throughput evaluation of performance in lignocellulose hydrolysates. *Bioresource Technol Rep* 2020;11:100532.
- Vowinckel J, Hartl J, Butler R et al. MitoLoc: a method for the simultaneous quantification of mitochondrial network morphology and membrane potential in single cells. *Mitochondrion* 2015;24:77–86.
- Wang B, Barahona M, Buck M. A modular cell-based biosensor using engineered genetic logic circuits to detect and integrate multiple environmental signals. *Biosens Bioelectron* 2013;40:368–76.
- Wang G, Øzmerih S, Guerreiro R et al. Improvement of cis, cis-muconic acid production in *Saccharomyces cerevisiae* through biosensor-aided genome engineering. *ACS Synth Biol* 2020;9:634–46.
- Wu Y, Chen T, Liu Y et al. Design of a programmable biosensor-CRISPRi genetic circuits for dynamic and autonomous dual-control of metabolic flux in *Bacillus subtilis*. *Nucleic Acids Res* 2020;48:996–1009.